ISBN: 978-3-95450-212-7 ISSN: 2673-5482 doi:10.18429/JACoW-CYCLOTRONS2022-MOP0014

DESIGN STUDIES OF THE CYLINDRICALLY SYMMETRIC MAGNETIC INFLECTOR

Lige Zhang*, Yi-Nong Rao, Rick Baartman, Yuri Bylinski, Thomas Planche
TRIUMF, Vancouver, BC, Canada

Abstract

The magnetic inflector is a promising alternative to achieve axial beam injection in a cyclotron with high beam energy. To demonstrate the technology, we use the TR100, a conceptual H2+ cyclotron, as a testbench to study the inflection conditions and optics of the passive magnetic inflector with a cylindrically symmetric structure. A mirror-like field with optimized mirror length and ratio provides a well-focused beam arriving at the median plane. The required magnetic field is produced by shimming a center plug in the injection hole. The space charge effect is also discussed with the simulation of a high-intensity injection beam.

INTRODUCTION

The spiral inflector steers the beam from the bore in the main magnet into the median plane to achieve the axial injection with an external ion source. In a conventional electrostatic inflector, the injection beam energy is limited by the breakdown voltage on the electrodes. While the injection intensity is also limited by the small aperture in the electrostatic inflector. Magnetic inflector is promising to overcome these disadvantages.

Recently, There are two types of magnetic inflector. One is the passive type which uses the iron in the injection hole to produce the required magnetic field. [1] The other is the active one which uses a permanent magnet array. [2] The passive type is more robust because there is no concern about the degaussing of the permanent magnet under the high beam loss in the injection hole. But it is only a concept, that has no existing design. To demonstrate the technology, we designed a magnetic inflector model for the conceptual H2+ cyclotron, TR100 [3]. The inflection conditions and focal properties of the passive magnetic inflector are studied using the particle tracking method. The preliminary simulation considering space charge is also discussed.

REFERENCE ORBIT

Motion Equations

In a cylindrically symmetric magnet. The magnetic vector potential A only consists of the azimuthal component A_θ. A_θ is the function of r and z. Thus, the hamiltonian is independent from θ, which is written as:

$$H = \sqrt{P_r^2c^2 + P_z^2c^2 + c^4m_0^2 + \frac{c^2\left(P_\theta - qr\,\mathrm{A}_\theta\,(r,z)\right)^2}{r^2}} \tag{1}$$

* lzhang@triumf.ca

where the canonical momenta are:

$$\begin{aligned} P_r &= p_r \\ P_\theta &= \gamma m_0 \theta' r^2 + qrA_\theta\,. \\ P_z &= p_z \end{aligned} \tag{2}$$

We can easily find that the canonical momentum in the azimuthal direction is a constant. Defining a potential function U with the constant azimuthal momenta and the magnetic vector potential as:

$$U = \frac{\left(P_\theta - qr\,\mathrm{A}_\theta\,(r,z)\right)^2}{2\gamma m_0 r^2} \tag{3}$$

the motion equation, essentially as obtained by Glaser [4], could be written in the following form:

$$\begin{aligned} P_r' &= \frac{\partial U}{\partial r} \\ P_\theta' &= 0 \\ P_z' &= \frac{\partial U}{\partial z} \end{aligned}\quad . \tag{4}$$

Substituting Eq. (2) into Eq. (4), the motion equation is written as:

$$\begin{aligned} \theta' &= \theta_0' r_0^2/r^2 + \frac{q}{\gamma m_0 r^2}(r_0\,\mathrm{A}_{\theta 0} - r\,\mathrm{A}_\theta) \\ \gamma m_0 r'' &- \frac{\partial U}{\partial r} = 0 \\ \gamma m_0 z'' &- \frac{\partial U}{\partial z} = 0 \end{aligned} \tag{5}$$

Because U is independent of θ and time t, the motion on the r-z plane is conservative. To find a proper reference orbit, we only need to solve the 2-D motion equation on the r-z plane.

Numerical Solution for a Mirror-like Magnetic Vector potential

The magnetic mirror is a component that is used to confine the charged particles. The particles inside a magnetic mirror are bounced back before the mirror point, in this paper we use a similar field to inflect the beam. The vector potential used to define the axial symmetric magnetic field in a mirror field is given as:

$$A_\theta = \frac{A_1\beta r}{2} - A_2 I_1(\beta r)\cos\beta z \tag{6}$$

where π/β is the mirror length, $\beta(A_1 + A_2)/(A_1 - A_2)$ is the mirror ratio.

ISBN: 978-3-95450-212-7 ISSN: 2673-5482 doi:10.18429/JACoW-CYCLOTRONS2022-MOP0014

The given magnetic field satisfies Laplace's equation, which ensures the curl of the magnetic field is zero. The linear approximation of the vector potential is given as:

$$A_{theta} = \frac{\beta r}{2}(A_1 - A_2 \cos \beta z)\,. \tag{7}$$

We use the TR100 main magnet model as a test bench to study the injection. The magnetic field in the central region is 2 T. The designed injection energy is around 35 keV. Figure 1(a) shows the conceptual model. By tracking the particle reversely from the median plane to the injection point with different Pitch angles, the different reference orbits are shown in Fig. 1 (b). Without breaking the median plane symmetry, the particle starting with 0 pitch angles on the median plane could not travel up to the injection point, which means we still need an electrostatic deflector on the median plane to fully steer the beam into the median plane. The single B_r bump field near the median plane could reduce the pitch angle by about 20° from the injection point to the median plane.

The final pitch angle on the median plane is around 20°, which only needs around 5 times less electrical field to fully steer the beam onto the median plane compared with a similar size inflector.

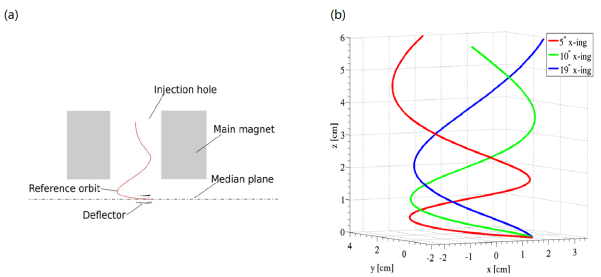

Figure 1: Reference orbit in the injection hole.

BEAM OPTICS

Coordinates Transformation

In this paper, we use the coordinate (α, β, γ) in the optical coordinate system, which moves along the reference orbit as shown in Fig. 2 [5]. The γ direction is the same as the velocity of the reference particle. The β direction is perpendicular to the γ direction and parallel to the median plane. At the same time, the cross product of the unit vector of the γ direction and β direction should have a positive projection on z-axis. The α direction is defined by the cross product of the unit vector of the γ direction and β direction.

The position vector $\vec{c}$ of the point on the reference orbit in cartesian is written as:

$$\vec{c} = (x_c(s), y_c(s), z_c(s)) \tag{8}$$

where s, the distance along the reference orbit, is the independent variable. The base vector $\vec{e} = (\vec{e_\alpha}, \vec{e_\beta}, \vec{e_\gamma})$ of the moving optical coordinate on the reference orbit is written as:

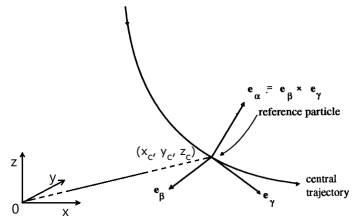

Figure 2: The moving optical coordinate system.

$$\begin{aligned} \vec{e_\alpha} &= (x_\alpha(s), y_\alpha(s), z_\alpha(s)) \\ \vec{e_\beta} &= (x_\beta(s), y_\beta(s), z_\beta(s)) \\ \vec{e_\gamma} &= (x_\gamma(s), y_\gamma(s), z_\gamma(s))\,. \end{aligned} \tag{9}$$

The transformation from cartesian coordinates (x, y, z) to the moving coordinates (α, β, γ) is written as:

$$\begin{aligned} x &= x_c(s) + \alpha x_\alpha(s) + \beta x_\beta(s) + \gamma x_\gamma(s) \\ y &= y_c(s) + \alpha y_\alpha(s) + \beta y_\beta(s) + \gamma y_\gamma(s) \\ z &= z_c(s) + \alpha z_\alpha(s) + \beta z_\beta(s) + \gamma z_\gamma(s)\,. \end{aligned} \tag{10}$$

Thus, the transformation matrix from the moving coordinates to the cartesian coordinates is:

$$\mathrm{M} = \begin{bmatrix} x_\alpha(s) & x_\beta(s) & x_\gamma(s) \\ y_\alpha(s) & y_\beta(s) & y_\gamma(s) \\ z_\alpha(s) & z_\beta(s) & z_\gamma(s) \end{bmatrix}\,. \tag{11}$$

The inverse transformation matrix $\mathrm{M}' = \mathrm{M}^T$, as the $(e_\alpha, e_\beta, e_\gamma)$ are orthogonal bases. Choosing a possible generating function that is consistent with Eq. (10).

$$\begin{aligned} G = &-P_x[x_c(s) + \alpha x_\alpha(s) + \beta y_\alpha(s) + \gamma z_\alpha(s)] \\ &- P_y[y_c(s) + \alpha x_\beta(s) + \beta y_\beta(s) + \gamma z_\beta(s)] \\ &- P_z[z_c(s) + \alpha x_\gamma(s) + \beta y_\gamma(s) + \gamma z_\gamma(s)]\,. \end{aligned} \tag{12}$$

The new canonical momenta is derived from the given generating function:

$$\begin{aligned} P_\alpha &= -\frac{\partial G}{\partial \alpha} = P_x x_\alpha(s) + P_y x_\beta(s) + P_z x_\gamma(s) \\ P_\beta &= -\frac{\partial G}{\partial \beta} = P_x y_\alpha(s) + P_y y_\beta(s) + P_z y_\gamma(s) \\ P_\gamma &= -\frac{\partial G}{\partial \gamma} = P_x z_\alpha(s) + P_y z_\beta(s) + P_z z_\gamma(s)\,. \end{aligned} \tag{13}$$

The canonical momenta under the cartesian coordinate system is given by:

$$\begin{aligned} P_x &= m_0 v_x + qA_x = m_0 v_0 x' + qA_x \\ P_y &= m_0 v_y + qA_y = m_0 v_0 y' + qA_y \\ P_z &= m_0 v_z + qA_z = m_0 v_0 z' + qA_z \end{aligned} \tag{14}$$

ISBN: 978-3-95450-212-7 ISSN: 2673-5482 doi:10.18429/JACoW-CYCLOTRONS2022-MOP0014

where the prime denotes differentiation with respect to s, v_0 is the velocity. Substitute Eq. (14) into Eq. (13), the new canonical momenta is written as

$$\begin{bmatrix} P_\alpha \\ P_\beta \\ P_\gamma \end{bmatrix} = m_0 v_0 \mathrm{M}^T \begin{bmatrix} x' \\ y' \\ z' \end{bmatrix} + q\mathrm{M}^T \begin{bmatrix} A_x \\ A_y \\ A_z \end{bmatrix}. \quad (15)$$

Substituting the coordinates on the reference orbit into Eq. (15), the canonical momenta on the reference trajectory is:

$$\begin{bmatrix} P_{\alpha 0} \\ P_{\beta 0} \\ P_{\gamma 0} \end{bmatrix} = m_0 v_0 \mathrm{M}^T \begin{bmatrix} x_c' \\ y_c' \\ z_c' \end{bmatrix} + q\mathrm{M}^T \begin{bmatrix} A_{x0} \\ A_{y0} \\ A_{z0} \end{bmatrix}. \quad (16)$$

To make the canonical variable small quantities, we subtract Eq. (16) from Eq. (15). Thus, the generating function becomes:

$$\begin{aligned} G = &-P_x[x_c(s) + \alpha x_\alpha(s) + \beta y_\alpha(s) + \gamma z_\alpha(s)] \\ &- P_y[y_c(s) + \alpha x_\beta(s) + \beta y_\beta(s) + \gamma z_\beta(s)] \\ &- P_z[z_c(s) + \alpha x_\gamma(s) + \beta y_\gamma(s) + \gamma z_\gamma(s)] \\ &+ \alpha P_{\alpha 0} + \beta P_{\beta 0} + \gamma P_{\gamma 0} \end{aligned}. \quad (17)$$

The new momenta is given by:

$$\begin{bmatrix} P_\alpha \\ P_\beta \\ P_\gamma \end{bmatrix} = m_0 v_0 \mathrm{M}^T \begin{bmatrix} x' - x_c' \\ y' - y_c' \\ z' - z_c' \end{bmatrix} + q\mathrm{M}^T \begin{bmatrix} A_x - A_{x0} \\ A_y - A_{y0} \\ A_z - A_{z0} \end{bmatrix}. \quad (18)$$

Using Eq. (10) and Eq. (18) expand the transform matrix M into a 6×6 matrix the transformation from (x, P_x, y, P_y, z, P_z) to $(\alpha, P_\alpha, \beta, P_\beta, \gamma, P_\gamma)$ is given by:

$$\begin{bmatrix} \alpha \\ P_\alpha \\ \beta \\ P_\beta \\ \gamma \\ P_\gamma \end{bmatrix} = \mathrm{M}^T \begin{bmatrix} x - x_c \\ m_0 v_0 (x' - x_c') \\ y - y_c \\ m_0 v_0 (y' - y_c') \\ z - z_c \\ m_0 v_0 (z' - z_c') \end{bmatrix} + q\mathrm{M}^T \begin{bmatrix} 0 \\ A_x - A_{x0} \\ 0 \\ A_y - A_{y0} \\ 0 \\ A_z - A_{z0} \end{bmatrix}. \quad (19)$$

Transfer Matrix

In order to calculate the transfer matrix, we need to run 6 particles with orthogonal initial coordinates and momenta in the magnetic inflector. After transforming the coordinates at the end of the orbit into the moving coordinates system with the unit (mm, mrad, mm, mrad, mm, mrad), the transfer matrix is calculated as:

$$\mathrm{R} = \begin{bmatrix} 1.99 & 0.15 & -1.68 & -0.02 & 0.38 & 0.13 \\ -5.02 & 0.19 & -0.23 & -0.18 & 3.87 & 0.21 \\ 0.58 & 0.02 & 0.84 & 0.03 & -0.55 & -0.01 \\ -13.80 & -0.37 & -8.08 & 0.39 & 1.94 & -0.64 \\ -0.03 & 0.04 & -0.30 & 0.02 & 0.61 & 0.10 \\ 5.32 & 0.22 & -12.48 & 0.27 & -5.43 & 0.86 \end{bmatrix} \quad (20)$$

Testing the symplectic of the transfer matrix,

$$\mathrm{R}^T\mathrm{JR} - \mathrm{J} = \begin{bmatrix} 0 & -0.004 & -0.026 & 0.036 & 0.008 & -0.008 \\ 0.004 & 0 & -0.015 & 0.001 & -0.003 & -0.000 \\ 0.026 & 0.015 & 0 & -0.002 & 0.001 & 0.004 \\ -0.036 & -0.001 & 0.002 & 0 & 0.001 & -0.001 \\ -0.008 & 0.003 & -0.001 & -0.001 & 0 & -0.001 \\ 0.008 & 0.000 & -0.004 & 0.001 & 0.001 & 0 \end{bmatrix} \quad (21)$$

where J is given as:

$$\mathrm{J} = \begin{bmatrix} 0 & 1 & 0 & 0 & 0 & 0 \\ -1 & 0 & 0 & 0 & 0 & 0 \\ 0 & 0 & 0 & 1 & 0 & 0 \\ 0 & 0 & -1 & 0 & 0 & 0 \\ 0 & 0 & 0 & 0 & 0 & 1 \\ 0 & 0 & 0 & 0 & -1 & 0 \end{bmatrix}. \quad (22)$$

The symplectic error is between 10^{-3} and 10^{-2}, which may be resulted from the non-linear of the motion and the noise when tracking the particles numerically.

Beam Envelopes

The beam envelope is studied in the $\alpha - \beta - \gamma$ moving frame. In previous study [6], we found that a proper beam focusing in both directions could be achieved by adjusting the mirror length and the mirror ratio. In this paper, an optimal magnetic inflector field with mirror length of 10 cm and mirror ratio of 2 is produced by carefully shimming the iron in the injection hole. The envelop and 3D trajectory in the designed magnetic inflector is shown in Fig. 5 (a).

MAGNET DESIGN

A 2D model is used to calculate the magnetic field in the injection hole. The sector structure is modelled by introducing the pseudo material which uses a lumped factor k to calculate the B-H curve, different k means different width ratios of the sectors. for a 4-sector magnet with a sector width of 45 degrees, k is 0.5. For the yoke, k is 1, thus the B-H curve is that of the real steel. Figure 3 shows the structure of the central plug that we used to optimize the mirror field in the injection hole. Figure 4 shows the magnetic field of the optimal magnet model.

HIGH INTENSITY SIMULATION

Figure 5 shows the Comsol simulation of the beam injection with considering space charge.

ISBN: 978-3-95450-212-7 ISSN: 2673-5482 doi:10.18429/JACoW-CYCLOTRONS2022-MOP0014

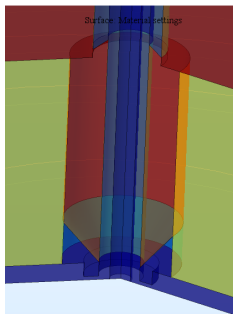

Figure 3: Steel plug in the injection hole. Blue colored material is the vacuum, green is the sector poles and red is the steel structure in the injection hole.

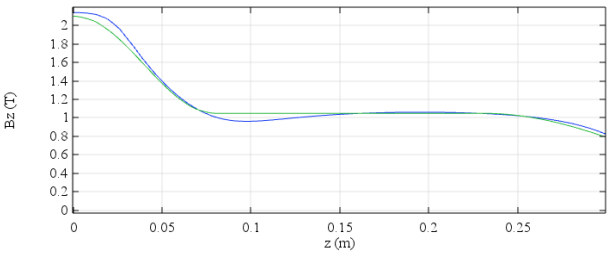

Figure 4: On-axis magnetic field in the injection hole after optimizing the shape of the center plug. The green line is the theoretic mirror field that could properly focus the beam in the inflector. Blue line is the on-axis magnetic field produced by the designed main magnet with a properly shimmed central plug.

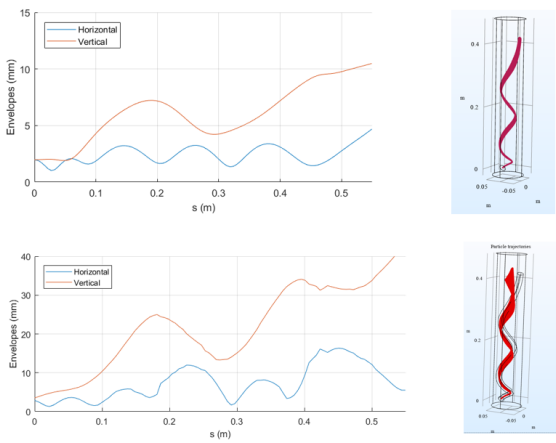

Figure 5: Envelope simulation considering space charge. The upper plots show the simulation a 1 nA injection beam. The lower one shows that of the 10 mA injection beam. The frame of a spiral pipe in the lower 3D beam plot shows the reference beam path without considering the space charge effect. Obviously, the reference orbit is changed by the space charge. A further design study of a shielding structure is needed to remove the repulsive force from different turns.

CONCLUSION

To maintain the median plane symmetry of the magnet, an electrostatic deflector should be placed at the end of the magnetic inflector, which will finally deflect the beam into the median plane with 0 vertical momenta. The required electric field strength in the electrostatic deflector is much lower than that in a conventional inflector. The envelope study suggests that the beam could be focused both horizontally and vertically in the moving frame under the optimized mirror ratio and mirror length. A steel plug in the center region is designed to produce the required field in the injection hole. A preliminary simulation of the high-intensity DC beam injection is simulated using Comsol, the reference orbit is changed by the space charge. Thus, a further design study of a shielding structure should be pursued.

ACKNOWLEDGEMENTS

This work was funded by TRIUMF which receives federal funding via a contribution agreement with the National Research Council of Canada.

REFERENCES

[1] W. Kleeven, “Injection and extraction for cyclotrons”, CERN Accelerator School, 2003.

[2] D. Winklehner *et al.*, “High power cyclotrons for neutrino experiments”, in *Proc. 5th Int. Particle Accelerator Conf.(IPAC’14)*, Dresden, Germany, Jun. 2014, pp. 788-–790.

[3] Y.-N. Rao, R. Baartman, Y. Bylinskii, T. Planche, and L. Zhang, ”Conceptual design of TR100+: an innovative superconducting cyclotron for commercial isotopes production”, in *Proc. 22nd Int. Conf. on Cyclotrons and their Applications (Cyclotrons’19)*, Cape Town, South Africa, Sep. 2019, pp. 298–301. doi:10.18429/JACoW-CYCLOTRONS2019-THB03

[4] W. Glaser, *Grundlagen der Elektronenoptik*, Springer-Verlag, 2013.

[5] R. Baartman and W. Kleeven, “A canonical treatment of the spiral inflector for cyclotrons”, *Part. Accel.*, vol. 41, pp. 41–53, 1993.

[6] D. Winklehner *et al.*, “Report of the Snowmass’21 Workshop on High-Power Cyclotrons and FFAs”, Mar 2022. doi:10.48550/ARXIV.2203.07919